

FAKE REN <sup>1,2</sup>, CHONGYANG WANG <sup>1,2,3\*</sup>, YISHA PAN <sup>4</sup>

### THE CORRELATION BETWEEN THE FLUID INJECTION PRESSURE AND THE UNIT FLUID INJECTION QUANTITY DURING HYDRAULIC FRACTURING

Hydraulic fracturing (HF) technology has been widely used in the coal mining industry. This technology can effectively increase the permeability coefficient of low-permeability coal seams, thereby enhancing the gas drainage efficiency and increasing the safety of coal mining. To study the correlation between the fluid injection pressure (FIP) and the unit fluid injection quantity (UFIQ) during hydraulic fracturing and considering the limitations of laboratory and numerical simulation methods, this study employs a field engineering experiment at the 1703 mining working face of Jin'zhong Coal Mine in Sichuan Province as the test site. Through the monitoring and analysis of the FIP and the UFIQ during the whole HF process of coal seam drilling, it is found that there is a certain correlation between the FIP and the UFIQ, the FIP will appear obvious "decreases-recovery" phenomenon when the coal cracks and cracks propagation. And in this process, the UFIQ will appear the corresponding "rise-recovery" phenomenon. At the same time, the fracturing process is divided into three stages according to the variation law of UFIQ in the HF process: liquid filling stage, energy storage and coal cracking cycle stage, and stop cracking stage. In addition, through the arrangement of holes stress gauges around the fracturing hole, it is found that the transfer of disturbance stress formed in the coal mass due to HF behavior is mainly attenuation, and its change stage in the whole HF process is mainly divided into the original stress stage, the stress response stage, and the stress stabilization stage. These results inform the design and optimization of fracturing parameters in hydraulic fracturing processes and aid in understanding the mechanisms of earthquake induction by HF.

**Keywords:** Hydraulic fracturing; fluid injection pressure; unit fluid injection quantity; correlation; disturbance stress

<sup>1</sup> CHONGQING UNIVERSITY, STATE KEY LABORATORY OF COAL MINE DISASTER DYNAMICS AND CONTROL, CHONGQING 400030, CHINA

<sup>2</sup> CHONGQING UNIVERSITY, SCHOOL OF RESOURCES AND SAFETY ENGINEERING, CHONGQING 400044, CHINA  
<sup>3</sup> POLITECNICO DI TORINO, DEPARTMENT OF STRUCTURAL, GEOTECHNICAL AND BUILDING ENGINEERING, TURIN, ITALY

<sup>4</sup> HENAN POLYTECHNIC UNIVERSITY, SCHOOL OF SURVEYING, MAPPING AND LAND INFORMATION ENGINEERING, JIAOZUO 454000, HENAN, CHINA

\* Corresponding author: 20212001033@cqu.edu.cn; wcy@cqu.edu.cn



## 1. Introduction

China is a large coal consumption country, and its coal is mainly from underground mining. Affected by geological conditions, most coal seams in China have complex occurrence conditions and poor permeability [1-3]. Resulting in low efficiency of coal seam gas extraction, which brings great difficulties to the safe mining of coal and coalbed methane (CBM). To safely and efficiently mine coal and CBM, scholars at home and abroad have carried out study further in this field in recent years. The research mainly focuses on how to increase the permeability of coal seams, including seepage mechanism research [4], crack mechanism research [5-6], fracture evolution law research [7-8], etc. According to the above research results, the coal seam permeability enhancement technology methods are: protective layer mining [9], deep hole loose blasting [10], hydraulic punching [11], hydraulic cutting [12], hydraulic fracturing [13], liquid CO<sub>2</sub> phase change fracturing [14], coal acidification [15], etc. In which HF technology has been more and more popularized and applied in recent years.

HF technology originated from a kind of in-situ stress measurement method and has a history of more than 70 years [16]. At first, HF technology was first applied to the natural gas and oil exploitation industries, mainly to increase the production capacity of oil and gas wells. In the later stage, with the rapid development of HF technology, the gradual deepening of CBM resource exploitation, the continuous improvement of its utilization technology and the increasingly serious gas disasters in the process of coal seam mining, HF technology has been gradually applied to coal and CBM exploitation [17].

The purpose of HF in coal seam is mainly to improve the extraction efficiency of coal seam gas by increasing the permeability of coal seam, to reduce the gas accidents in coal seam mining and ensure the safety of coal production. The technical principle is that by drilling in coal seam and injecting high-pressure liquid into the holes with the help of high-pressure pump, the stress state of holes wall and surrounding coal mass will change under the action of high-pressure liquid. When the liquid pressure in the holes exceeds the minimum principal stress existing in the coal mass itself, the phenomenon of holes wall cracking and crack propagation will occur. The crack propagation direction is generally parallel to the maximum principal stress direction. After HF of coal seam, the fracture density in coal mass increases, which effectively improves the connectivity of fracture network in coal mass, thereby improving the permeability of coal seam.

At present, on the study of coal seam HF technology, in the study of fracturing parameters change rule, Hu et al. [18] through the physical simulation test of coal HF in the laboratory, the HF is divided into four stages: filling with liquid, boosting pressure, lowering pressure and stabilizing pressure; Zhuang et al. [19] carried out hydraulic fracturing test by using six different injection schemes in the laboratory, and found that the cyclic pulse pressurization scheme had the best fracturing effect. Kumari et al. [20] obtained the relationship between rock initiation pressure and rock temperature and confining pressure by simulating rock HF test under high temperature and high pressure in laboratory. Ito and Hayashi [21] studied the flow law of fracturing fluid by using structural mechanics and coal-rock fluid theory and predicted the fracture size by using matrix fracture system to study and analyze the stress distribution near the fracturing holes. Through the research method of numerical simulation, Zhang et al. [22] found that the exploitation of filling wells after HF can change the local pore pressure and the stress field around the dilution zone. In the study of dynamic characteristics of HF, Lin et al. [23] employed a series of laboratory HF experiments and divided HF into three sections based on the crack expansion process: crack initiation, crack propagation, and crack closure stages. Zhang et al. [24] divided

the HF process into three stages according to the damage degree and permeability change of coal rock through experiments in the laboratory: coal rock compaction stage, coal rock expansion stage and coal rock fracture stage. Shan et al. [25] divided the HF into five stages: preparation, pressurization, fracture, crack propagation and post-fracture according to the pump pressure and crack propagation in the HF test in the laboratory.

From these studies, most studies are related to the FIP parameters in the process of HF, but there are few studies on the fluid injection quantity (FIQ) parameters, and there are few analyses and research on the change of FIQ in the whole HF process. At the same time, there is no unified standard and rule for the division of the whole HF process; in addition, most of the research methods are laboratory or computer numerical simulation, which lacks the verification of engineering application. Based on this, this study takes the 1703 mining working face of Jin'zhong Coal Mine as the engineering test site, through the HF test of coal seam to study the variation law and correlation of fracturing parameters in the whole HF process, and according to the change of UFIQ, the whole HF process is divided into three stages. At the same time, the holes stress gauge is arranged around the fracturing holes to monitor and analyze the variation law of disturbance stress formed in coal due to HF.

## 2. Materials and methods

### 2.1. Theoretical analysis on variation law of coal cracking related parameters

#### 2.1.1. Calculation of initiation pressure of inclined holes wall

Taking China Coal Mine as an example, the upward ventilation is often used in the coal mining working face, and the so-called upward ventilation is mainly due to the level of intake airflow roadway in coal mining face is lower than that of return laneway, resulting in airflow flowing from intake airflow roadway to return laneway along the inclined direction of coal seam (Fig. 1). Therefore, whether the coal seam drilling is constructed in the direction of return laneway to the intake airflow roadway or in the direction of intake airflow roadway to the return laneway, the coal seam drilling is inclined drilling.

To analyze the stress around the inclined drilling conveniently, the in-situ stress inside the coal seam can be transformed into the axial and radial stress distribution of the inclined drill-

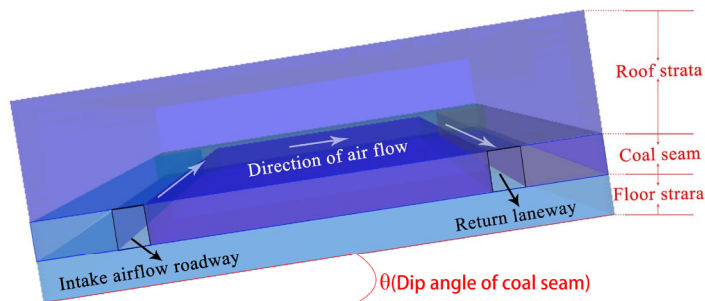


Fig. 1. Schematic diagram of upward ventilation mode of coal mining working face

ing. Accordingly, the three-dimensional Cartesian coordinate system  $(x, y, z)$  was established. Where the O-Z axis corresponds to the central axis of the inclined drilling, and the O-Y axis and the O-X axis are located on the plane perpendicular to the O-Z axis. In addition, to illustrate the stress situation more clearly at a certain point in the inclined drilling, the coordinate system  $(\sigma_v, \sigma_H$  and  $\sigma_h)$  consistent with the direction of the three-way principal geo-stress was established [26]. After unifying the two coordinate systems (Fig. 2), the following stress transformation equation can be obtained:

$$\begin{cases} \sigma_x = (\sigma_H \cos^2 \alpha + \sigma_h \sin^2 \alpha) \cos^2 \beta + \sigma_v \sin^2 \beta \\ \sigma_y = \sigma_H \sin^2 \alpha + \sigma_h \cos^2 \alpha \\ \sigma_z = (\sigma_H \cos^2 \alpha + \sigma_h \sin^2 \alpha) \sin^2 \beta + \sigma_v \cos^2 \beta \end{cases} \quad (1)$$

where  $\sigma_v$ ,  $\sigma_H$  and  $\sigma_h$  are the stress components of the holes cross-section coordinate system;  $\alpha$  is the angle between the holes azimuth and  $\sigma_H$ ;  $\beta$  is the angle between the holes central axis and  $\sigma_v$ .

Assuming that in the process of HF of coal seam drilling, under the action of high-pressure liquid and original stress, a certain point of the holes wall of coal seam drilling is cracked, the stress distribution of the section at this time can be regarded as a plane strain problem (Fig. 3).

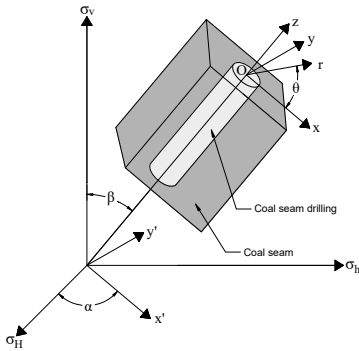


Fig. 2. Coordinate transformation of central axis of coal seam drilling

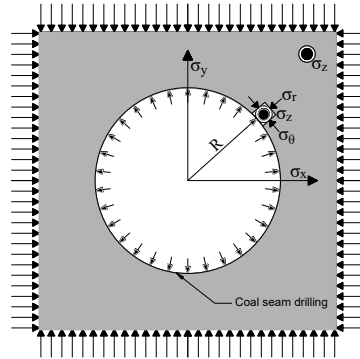


Fig. 3. Radial stress distribution of holes wall in coal seam

The stress distribution of holes wall can be obtained by superposition of high-pressure liquid and holes radial stress. Currently, the calculation Formula of stress distribution at a certain point of holes wall is as follows:

$$\begin{cases} \sigma_r = \frac{\sigma_x + \sigma_y}{2} \left(1 - \frac{R^2}{r^2}\right) + \frac{\sigma_x - \sigma_y}{2} \left(1 - \frac{4R^2}{r^2} + \frac{3R^4}{r^4}\right) \cos 2\theta + \frac{pR^2}{r^2} \\ \sigma_\theta = \frac{\sigma_x + \sigma_y}{2} \left(1 + \frac{R^2}{r^2}\right) - \frac{\sigma_x - \sigma_y}{2} \left(1 + \frac{3R^4}{r^4}\right) \cos 2\theta - \frac{pR^2}{r^2} \end{cases} \quad (2)$$

where  $\sigma_r$  and  $\sigma_\theta$  are radial stress and tangential stress at any point in the surrounding rock of holes wall in coal seam.  $R$  is the radius of the holes;  $r$  is the distance from any point to the holes center;  $\theta$  is the direction angle of any point in holes wall rock of coal seam;  $p$  is the pressure of liquid.

The Formula (1) is substituted into the Formula (2) to obtain the stress distribution of a point in the radial coal mass along the holes under the combined action of three-way geo-stress and high-pressure liquid:

$$\left\{ \begin{array}{l} \sigma_r = \left[ \frac{(\sigma_H \cos^2 \alpha + \sigma_h \sin^2 \alpha) \cos^2 \beta + \sigma_v \sin^2 \beta}{2} + \frac{\sigma_H \sin^2 \alpha + \sigma_h \cos^2 \alpha}{2} \right] \left( 1 - \frac{R^2}{r^2} \right) \\ \quad \left[ \frac{(\sigma_H \cos^2 \alpha + \sigma_h \sin^2 \alpha) \cos^2 \beta + \sigma_v \sin^2 \beta}{2} - \frac{\sigma_H \sin^2 \alpha + \sigma_h \cos^2 \alpha}{2} \right] \\ \quad \left( 1 - \frac{4R^2}{r^2} + \frac{3R^4}{r^4} \right) \cos 2\theta + \frac{pR^2}{r^2} \\ \sigma_\theta = \left[ \frac{(\sigma_H \cos^2 \alpha + \sigma_h \sin^2 \alpha) \cos^2 \beta + \sigma_v \sin^2 \beta}{2} + \frac{\sigma_H \sin^2 \alpha + \sigma_h \cos^2 \alpha}{2} \right] \left( 1 + \frac{R^2}{r^2} \right) - \\ \quad \left[ \frac{(\sigma_H \cos^2 \alpha + \sigma_h \sin^2 \alpha) \cos^2 \beta + \sigma_v \sin^2 \beta}{2} - \frac{\sigma_H \sin^2 \alpha + \sigma_h \cos^2 \alpha}{2} \right] \\ \quad \left( 1 + \frac{3R^4}{r^4} \right) \cos 2\theta - \frac{pR^2}{r^2} \end{array} \right. \quad (3)$$

According to the tensile strength of coal and rock mass is far less than its compressive strength, the coal cracking at the holes wall of coal seam should conform to the maximum tensile stress theory. Therefore, under the combined action of three-way geo-stress and high-pressure liquid, when the tensile stress at a certain position of the holes wall ( $r = R$ ) of coal seam exceeds the tensile strength of coal mass, the holes wall of coal seam will crack, that is, the pressure of high-pressure liquid acting on the holes wall needs to overcome the tangential stress of coal mass at the holes wall to cause tensile damage to the holes wall [27]. At this time, the stress state at a certain point in the holes wall can be expressed as:

$$\begin{aligned} \sigma_\theta = & \left[ (\sigma_H \cos^2 \alpha + \sigma_h \sin^2 \alpha) \cos^2 \beta + \sigma_v \sin^2 \beta + \sigma_H \sin^2 \alpha + \sigma_h \cos^2 \alpha \right] - \\ & 2 \left[ (\sigma_H \cos^2 \alpha + \sigma_h \sin^2 \alpha) \cos^2 \beta + \sigma_v \sin^2 \beta - \sigma_H \sin^2 \alpha - \sigma_h \cos^2 \alpha \right] \\ & \cos 2\theta - p \end{aligned} \quad (4)$$

To simplify the calculation, it is assumed that the maximum horizontal principal stress in the coal mass is parallel to the central axis of the holes, and the direction of the minimum principal stress is perpendicular to the direction of the maximum principal stress. Therefore, when the

holes wall of coal seam breaks along the radial direction of holes, the influence of radial stress of holes can be ignored, so the above equation can be simplified as:

$$\sigma_{\theta} = (\sigma_H \cos^2 \beta + \sigma_v \sin^2 \beta + \sigma_h) - 2(\sigma_H \cos^2 \beta + \sigma_v \sin^2 \beta - \sigma_h) \cos 2\theta - p \quad (5)$$

According to Formula 5, when  $\theta \in [0^\circ, 180^\circ]$ , if and only if  $\theta = 0^\circ$  and  $\theta = 90^\circ$ , the tangential stress at the holes wall of coal seam will reach the limit. Therefore, in both cases, the tangential stress at the holes wall of the coal seam only needs to consider the direction angle and extreme value:

$$\begin{cases} \sigma_{\theta=0} = 3\sigma_h - \sigma_H \cos^2 \beta - \sigma_v \sin^2 \beta - p \\ \sigma_{\theta=90} = 3(\sigma_H \cos^2 \beta + \sigma_v \sin^2 \beta) - \sigma_H - p \end{cases} \quad (6)$$

It is assumed that the tensile strength of the coal mass at the holes wall of the coal seam is  $\sigma_b$ , so to crack the coal mass at the holes wall of the coal seam,  $|\sigma_{\theta}| \geq \sigma_b$  must be satisfied. Based on this, the calculation Formula of  $p$  acting on the holes wall by high pressure liquid is obtained:

$$\begin{cases} p_{\theta=0} \geq 3\sigma_h - \sigma_H \cos^2 \beta - \sigma_v \sin^2 \beta + \sigma_b \\ p_{\theta=90} \geq 3(\sigma_H \cos^2 \beta + \sigma_v \sin^2 \beta) - \sigma_H + \sigma_b \end{cases} \quad (7)$$

Therefore, when the crack at the holes wall of coal seam extends along the radial direction, the initiation pressure  $p_s$  of the holes wall of coal seam can be expressed as:

$$p_s \geq \min \begin{cases} 3\sigma_h - \sigma_H \cos^2 \beta - \sigma_v \sin^2 \beta + \sigma_b \\ 3(\sigma_H \cos^2 \beta + \sigma_v \sin^2 \beta) - \sigma_H + \sigma_b \end{cases} \quad (8)$$

It can be seen from Formulas 8 that the initiation pressure  $p_s$  is a function of angle  $\beta$ . Therefore, the initiation position  $L_f$  of cracks in holes of inclined coal seam can be obtained by derivation of  $\beta$ , the initiation position  $L_f$  can be obtained by the following Formula:

$$\begin{cases} \frac{\partial p_s}{\partial \beta} = 0 \\ \frac{\partial^2 p_s}{\partial \beta^2} > 0 \end{cases} \quad (9)$$

### 2.1.2. Variation law of FIP in coal cracking moment

After the coal seam drilling cracks under the action of high-pressure liquid, the high-pressure liquid enters the bedding surface and fracture system in the coal mass driven by the high-pressure pump, and acts on the weak surface to cut the coal fracture [28,29]. This will lead to the expansion of coal in space and promote the expansion and extension of the weak surface, gradually forming interconnected fracture network in coal, and further causing the fracturing decomposition

of coal. According to the state equation of pure fluid, when any two of  $P$ ,  $V$  and  $T$  are specified, the state will be determined. The corresponding mathematical equation is :

$$f(P, V, T) = 0 \quad (10)$$

The ideal gas state equation can be described as:

$$PV = nRT \quad (11)$$

where  $P$  is the pressure, Pa;  $V$  is the volume of gas,  $\text{m}^3$ ;  $T$  is temperature, K;  $n$  is the amount of substance of gas, mol;  $R$  is a molar gas constant,  $\text{J}/(\text{mol} \cdot \text{K})$ .

The corresponding liquid state equation can be described as:

$$V(T, P) = V_0 [1 + \alpha_f(T - T_0) - \beta_f P] \quad (12)$$

where  $\alpha_f$  is the expansion coefficient of liquid;  $\beta_f$  is the compressibility coefficient of liquid;  $V_0$  is the volume of fluid at temperature  $T_0$ ,  $\text{m}^3$ .

From the above equation, the increase of fluid volume and the decrease of temperature will lead to the decrease of fluid pressure. For HF of underground coal seam, the change of fracturing fluid temperature  $T$  is negligible. Therefore, in the moment of coal cracking, the water filling space inside the coal will suddenly increase with the coal cracking and crack expansion. It can be considered that the volume of high-pressure liquid will suddenly increase, and the corresponding high-pressure liquid in the whole fracturing system will have a short “pressure relief” phenomenon, this is mainly because: 1) the instantaneous increase of water filling space; 2) Fracturing fluid cannot be replenished in time. However, with the continuous operation of the high-pressure pump, the external fracturing fluid will continue to be added to the coal mass, and then gradually compensate the “loss” of the previous FIP, so that the FIP inside the coal mass can be “restored”; And when the pressure of the fracturing fluid at the end of the fracture reaches the initiation pressure of the coal, the coal will crack again.

### 2.1.3. Variation law of FIQ in coal cracking moment

In the process of coal fracturing, the mechanical energy of the fracturing fluid mainly comes from the high-pressure pump. Assuming that the mechanical energy of the fluid on a section in the fracturing holes now of coal cracking is  $E$ , then according to the Bernoulli equation, it can be obtained:

$$P + \frac{\rho v^2}{2} + \rho gh = E \quad (13)$$

where  $P$  is the pressure at a certain point in the fluid, Pa;  $\rho$  is fluid density,  $\text{kg}/\text{m}^3$ ;  $v$  is the flow velocity of the fluid at this point,  $\text{m}/\text{s}$ ;  $g$  is the gravity acceleration,  $\text{m}/\text{s}^2$ ;  $h$  is the height of the point,  $\text{m}$ .

As described in sub-section 2.1.2, coal cracking increases its internal water filling space, resulting in a certain degree of “pressure relief” of FIP. According to the law of conservation of mass, now of coal cracking, for the fluid on the same cross-section, its mechanical energy  $E$  has not changed, and its density  $\rho$  and its own gravitational potential energy have not changed,

so when its pressure  $P$  decreases, its velocity  $v$  will increase, resulting in an increase in FIQ during this period. In other words, in coal cracking moment, with the decrease of FIP, the injection rate will increase. Further analysis shows that the FIQ required for the fracturing fluid in the holes after coal cracking is “restoring” its own pressure, which includes two parts: 1) the FIQ required for filling the cracking space; 2) The amount of liquid injection needed to infiltrate the coal around the fracture and its capillary effect. With the continuous work of the high-pressure pump, the corresponding FIQ will be supplemented within a certain period, so that the FIP in the coal mass will be restored, and then the injection rate will decrease. At the same time, with the increase of fluid injection volume and mechanical energy of fracturing fluid, the coal will crack again when the pressure of fracturing fluid at the end of the crack reaches the starting pressure of coal.

## 2.2. Experimental location

The HF test location of coal seam is in Jin’zhong Coal Mine, Sichuan Province, China (Fig. 4). According to the actual conditions in the Coal Mine, 1703 mining working face was selected as the experimental working face, and 7<sup>#</sup> coal seam was mined in this working face. The gas content, gas pressure and permeability coefficients were 4.48 m<sup>3</sup>/t, 0.37 MPa and 0.37 m<sup>2</sup>, respectively; The strike length of 1703 working face is 480 m (360 m already mined), the dip length is 120 m, and the dip angle of coal seam is 14°; the working face adopts longwall backward mining method and all caving method to manage the roof of goaf; the average thickness of 7<sup>#</sup>

TABLE 1

List of roof and floor conditions of 1703 coal face

Name of roof and floor	Name of coal rock	Thickness (m)	Roof and floor characteristics
Main roof	Sandstone	3.00	The roof is sandy mudstone, fine sandstone, and argillaceous siltstone, belonging to medium to hard rock mass, and the roof is stable ; floor is sandstone, sandy mudstone, clay rock, clay rock, mudstone, belongs to unstable, soft rock mass
Immediate roof	Mudstone	1.00	
false roof	Carbon mudstone	0.30	
	7 <sup>#</sup> coal seam	1.40	
Immediate floor	Mudstone	0.20	
Main floor	Shaly Sand	2.00	

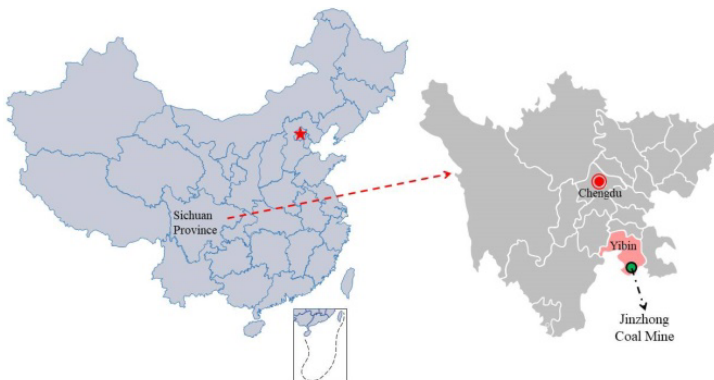


Fig. 4. Location of experiment site

coal seam in 1703 mining working face is 1.40 m, and the roof and floor are shown in TABLE 1. At present, a certain number of bedding gas drainage holes have been constructed in 1703 mining working face (Fig. 5).

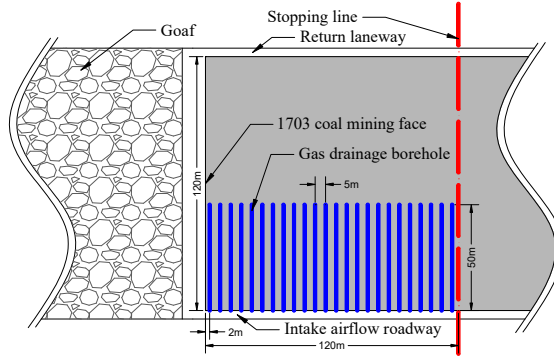


Fig. 5. Distribution of gas drainage holes in 1703 coal face

### 2.3. Experiment equipment

The equipment used in this HF test mainly includes BRW200/31.5 emulsion pump, water tank matched with emulsion pump, high-pressure capsule hole packer, high-pressure glue pipe, fracturing rod, pressure meter flowmeter and so on. The physical picture of each component is shown in Fig. 6, and the overall connection diagram is shown in Fig. 7.

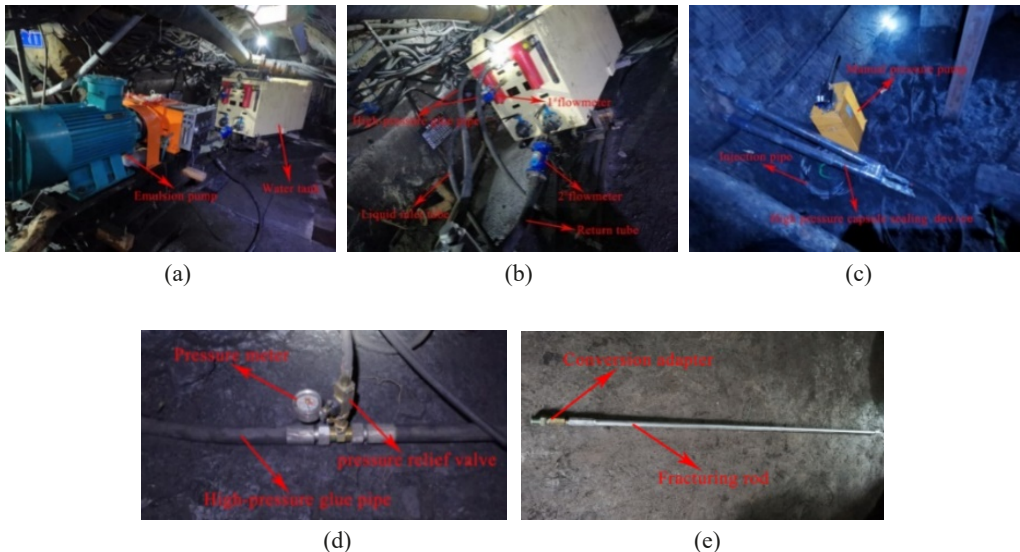


Fig. 6. Physical pictures of various components of hydraulic fracturing equipment. (a) Pump set; (b) Pipeline and flowmeter; (c) Hole packer; (d) pressure meter; (e) Fracturing rod

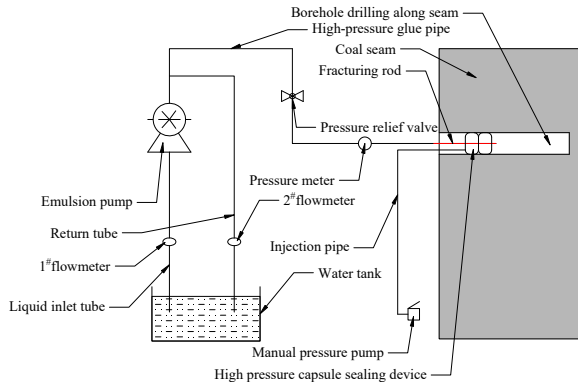


Fig. 7. Connection diagram of hydraulic fracturing equipment

## 2.4. Experiment scheme

### 2.4.1. Underground equipment layout

According to the actual conditions of Jin'zhong Coal Mine, due to the small cross-sectional area of the roadway connected with the intake airflow roadway and return laneway of the 1703 mining working face, the pump group needed for HF cannot be passed. Therefore, the pump group is arranged in the roadway near the central substation of the 1703 mining working face, and the pump group relates to the fracturing holes through the high-pressure glue pipe. The underground location of the pump group is shown in Fig. 8.

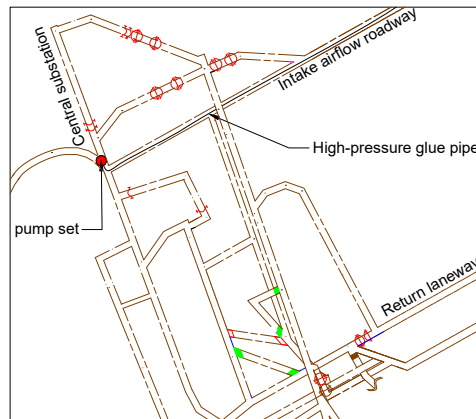


Fig. 8. Location diagram of underground pump set

### 2.4.2. Holes layout

According to the experimental purpose and the actual conditions of 1703 mining working face in Jin'zhong Coal Mine, and combined with the actual needs of the mine, three HF holes,

three disturbance stress monitoring holes and two control holes were arranged in 1703 mining working face. Affected by the roadway maintenance and pipeline installation in the return laneway, each hole was constructed along the coal seam to the return laneway in the intake airflow roadway. The construction parameters and layout of each hole are shown in TABLE 2 and Fig. 9. The role of 1<sup>#</sup> control hole and 2<sup>#</sup> control hole is to observe the fracturing range of 1<sup>#</sup> fracturing hole and 2<sup>#</sup> fracturing hole, respectively; 1~3<sup>#</sup> stress monitoring holes are mainly used to monitor the change of disturbance stress in the surrounding coal mass of 3<sup>#</sup> fracturing hole during the whole HF process.

TABLE 2

Construction parameters of each hole

Name	Hole diameter (mm)	Hole depth (mm)	Inclination (°)	Remark
1 <sup>#</sup> fracturing hole	75	90	14	Sealing depth 80 m
2 <sup>#</sup> fracturing hole	75	90	14	Sealing depth 80 m
3 <sup>#</sup> fracturing hole	75	90	14	Sealing depth 80 m
1 <sup>#</sup> control hole	75	90	14	No sealing
2 <sup>#</sup> control hole	75	90	14	No sealing
1 <sup>#</sup> stress monitoring hole	75	80	14	Sealing depth 80 m
2 <sup>#</sup> stress monitoring hole	75	80	14	Sealing depth 80 m
3 <sup>#</sup> stress monitoring hole	75	80	14	Sealing depth 80 m

**2.4.3. Regulation schemes of FIP**

During the HF of coal seam, it is necessary to continuously adjust the FIP in the whole HF process, to continuously supplement energy for high-pressure liquid to crack the coal mass, thereby improving the permeability enhancement efficiency of coal seam. According to the above analysis of holes wall initiation pressure in coal seam and the reference to the whole HF operation process of adjacent mines, the regulation schemes of FIP in the HF test of 1307 working face in Jin'zhong Coal Mine is shown in Fig. 10.

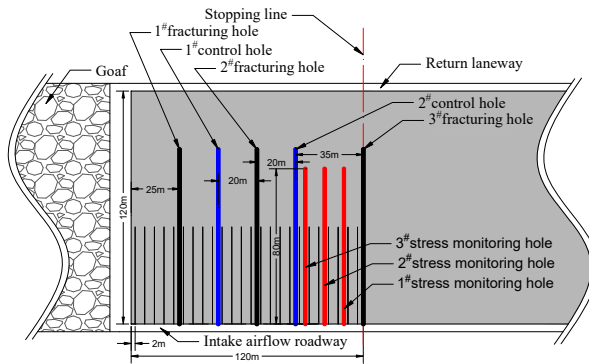


Fig. 9. Layout of each hole

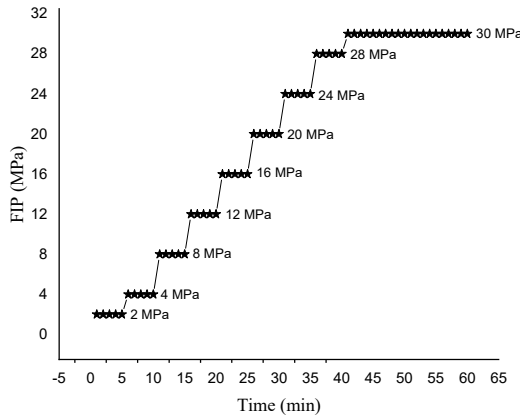


Fig. 10. Regulation scheme of FIP

### 3. Results and analysis

#### 3.1. Calculation of UFIQ

The flowmeters used in this HF process are installed in the liquid inlet and return tube between the emulsion pump and the water tank (Fig. 3b). The 1<sup>st</sup> flowmeter is installed on the liquid inlet tube, and the flow value detected is  $Q_{in}$ . The value of  $Q_{in}$  represents the flow from the water tank to the emulsion pump. The 2<sup>nd</sup> flowmeter is installed on the return tube, and the flow value is  $Q_{out}$ . The value of  $Q_{out}$  represents the flow returned from the emulsion pump to the water tank. In the process of HF, after the fracturing fluid in the water tank enters the emulsion pump, only part of the fracturing fluid enters the coal seam drilling through the high-pressure pipe under the pressure of the emulsion pump, and the other part of the fracturing fluid returns to the water tank through the return tube. Therefore, the actual FIQ in the process of HF is the difference between  $Q_{in}$  and  $Q_{out}$  :

$$Q = Q_{in} - Q_{out} \quad (14)$$

where  $Q$  is the actual FIQ during HF,  $m^3$ ;  $Q_{in}$  is the flow of liquid inlet tube,  $m^3$ ;  $Q_{out}$  is the flow of return tube,  $m^3$ .

To facilitate the processing and analysis of fracturing fluid flow data, this paper introduces unit liquid flow, it is the liquid flow through each tube in one minute. Therefore, the unit liquid flow of the liquid inlet tube, the unit liquid flow of the return tube and the actual unit liquid flow in a certain minute are:

$$\left\{ \begin{array}{l} Q_{unit}^t(in) = Q_{unit}^t(in) - Q_{unit}^{t-1}(in) \\ Q_{unit}^t(out) = Q_{unit}^t(out) - Q_{unit}^{t-1}(out) \\ Q_{unit}^t(fact) = Q_{unit}^t(in) - Q_{unit}^{t-1}(in) - (Q_{unit}^t(out) - Q_{unit}^{t-1}(out)) \end{array} \right. \quad (15)$$

where  $Q_{unit}^{i(fact)}$  is the actual unit liquid flow through the high-pressure pipeline at  $i$  minute,  $m^3$ ;  $Q_{unit}^{i(in)}$  and  $Q_{unit}^{i-1(in)}$  are the unit liquid flow through the liquid inlet tube at  $i$  minute and  $i-1$  minute,  $m^3$ ;  $Q_{unit}^{i(out)}$  and  $Q_{unit}^{i-1(out)}$  are the unit liquid flow through the return tube at  $i$  minute and  $i-1$  minute,  $m^3$ .

### 3.2. Variation law of fracturing fluid flow value

According to the above HF experiment scheme, HF is carried out for 1<sup>#</sup> fracturing hole, 2<sup>#</sup> fracturing hole, and 3<sup>#</sup> fracturing hole respectively. When the 1<sup>#</sup> fracturing hole is fractured to 41 minutes, the flow phenomenon occurs in the 1<sup>#</sup> control hole. With the increasing flow of the 1<sup>#</sup> control hole, the HF stops at 45 minutes. 2<sup>#</sup> fracturing hole in fracturing to 42 minutes, 2<sup>#</sup> control hole appears flow phenomenon, so also in fracturing to 45-minute stop HF; the 3<sup>#</sup> fracturing hole was fractured for 90 minutes, in which the FIP remained at 30 MPa during 45~90 minutes, and the 2<sup>#</sup> control hole with a distance of 35 m did not flow until the end of the HF. To effectively illustrate the change rule of liquid flow in each pipeline during HF, the unit liquid flow value of each pipeline is sorted out and the corresponding line chart is drawn. Among them, 1~2<sup>#</sup> fracturing holes in the HF process of each pipeline unit liquid flow value change rule as shown in Fig. 11, 3<sup>#</sup> fracturing hole in the HF process of each pipeline unit liquid flow value change rule as shown in Fig. 12.

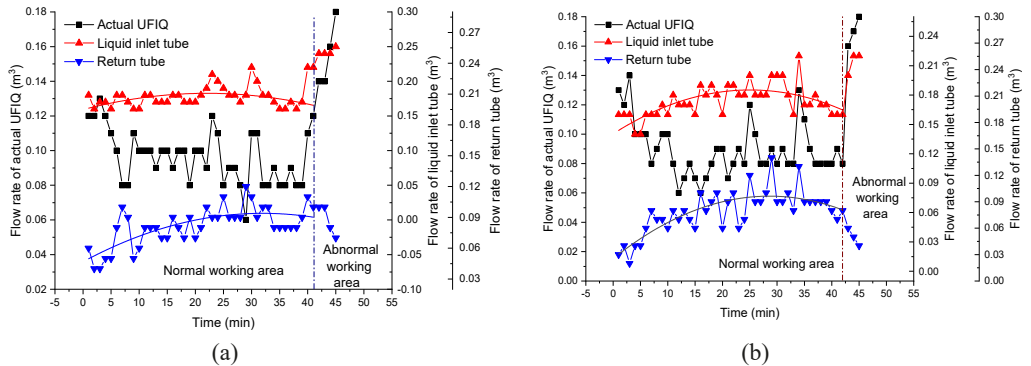


Fig. 11. Curve diagram of unit flow rate variation of 1~2<sup>#</sup> fracturing holes during HF.  
 (a) 1<sup>#</sup> fracturing holes; (b) 2<sup>#</sup> fracturing holes

It can be seen from Fig. 11 that in the whole HF process of 1~2<sup>#</sup> fracturing holes, the two fracturing holes have experienced the process of coal cracking, crack propagation and the flow of corresponding control holes. Therefore, the variation of unit liquid flow rate in the whole HF process of 1~2<sup>#</sup> fracturing holes is divided into normal working area (corresponding control holes do not appear flow phenomenon) and abnormal working area (corresponding control holes appear flow phenomenon). The 1<sup>#</sup> fracturing hole is in the stage of coal cracking and crack propagation in 0~40 minutes. After fracturing to 40 minutes, the 1<sup>#</sup> control hole has appeared flow phenomenon, and the flow is getting larger and larger, so the fracturing of 1<sup>#</sup> fracturing hole is stopped at 45 minutes. The 2<sup>#</sup> fracturing hole is in the stage of coal cracking and crack

propagation within 0~43 minutes. After fracturing to 43 minutes, the 2<sup>#</sup> control hole appears the phenomenon of water flow. To reduce the use of fracturing fluid, the fracturing of 2<sup>#</sup> fracturing hole is also stopped at 45 minutes. In addition, the right side of the 1<sup>#</sup> fracturing holes is 20 m away from the 1<sup>#</sup> control holes, and the left side is 25 m away from the working face. Because of the influence of mining disturbance, there will be a certain range of fracture development zones in the working face along the advancing direction [30]. During the whole HF process of the 1<sup>#</sup> fracturing hole, only the flow phenomenon occurs in the 1<sup>#</sup> control hole, while the flow and related signs are not seen in the coal wall of the working face, indicating that during the HF process of the 1<sup>#</sup> fracturing hole, the crack propagation of the coal on both sides is uneven and asymmetric. Correspondingly, the left side of the 2<sup>#</sup> fracturing hole is 20 m away from the 1<sup>#</sup> control hole, and the right side is 20 m away from the 2<sup>#</sup> control hole. In the whole HF process of the 2<sup>#</sup> fracturing hole, the flow phenomenon only occurs in the 2<sup>#</sup> control hole, and there is no flow phenomenon in the 1<sup>#</sup> control hole. It also proves that the unevenness and asymmetry of coal crack propagation on both sides of the fracturing holes in the HF process.

In addition, it can also be seen from the figure that the unit liquid flow rate of the liquid inlet tube of 1~2<sup>#</sup> fracturing holes is in the normal working area. After data fitting, the trend of the curve is “parabola” rather than “straight line”, indicating that the unit liquid flow rate of the liquid inlet tube does not increase linearly with the increasing FIP. In the abnormal working area, the unit liquid flow rate of the liquid inlet tube of 1~2<sup>#</sup> fracturing holes shows a rapid growth trend in a short period of time. The main reason is that the continuous expansion of coal cracks under the action of FIP leads to the continuous increase of water filling space and the decrease of water flow resistance. At the same time, the unit liquid flow rate of the return tube of the 1~2<sup>#</sup> fracturing holes is in the normal working area. After data fitting, the trend of the curve is also “parabolic”. In the abnormal fracturing area, the unit liquid flow rate of the return pipe of 1~2<sup>#</sup> fracturing holes shows a rapid decline trend in a short period of time. The main reason is that after the communication between the fracturing holes and the control holes, the flow resistance decreases rapidly, which improves the liquid injection efficiency of the emulsion pump. In addition, it can be seen from the Fig. 8 that the variation trend of actual UFIQ of 1~2<sup>#</sup> fracturing holes can be described as three stages in the whole HF process : the decline stage, the fluctuation stage, and the rise stage. The initial stage of HF is mainly manifested as an obvious decline stage. In the first one minute of the beginning of HF, it is necessary to inject liquid into the space of the high-pressure pipeline, the fracturing hole, and the fractures around the borehole in this period. Therefore, the actual UFIQ in this period is relatively high, and then the fracturing fluid in the fracturing hole enters the energy storage stage. At this time, the actual UFIQ will be significantly reduced. The 1<sup>#</sup> fracturing hole and the 2<sup>#</sup> fracturing hole are in the decline stage during the first 0~6 minutes and the first 0~7 minutes fracturing, respectively. The fluctuation stage is mainly manifested in the decline stage and before the communication between the fracturing holes and the control holes. The most obvious characteristic of the actual UFIQ in the fluctuation stage is the instability of its flow value, which should be mainly due to the cracking and crack propagation of coal mass. The rise stage is mainly after the communication between the fracturing holes and the control holes, after the flow phenomenon occurs in the control hole, due to the continuous expansion and increase of the communication cracks, as well as the rapid increase of the unit liquid flow in the liquid inlet tube and the rapid decrease of the unit liquid flow in the return tube, the actual UFIQ of the fracturing hole also shows a rapid upward trend.

It can be seen from Fig. 12 that the overall change of unit liquid flow in each pipeline of 3<sup>#</sup> fracturing hole is slightly different from that of 1~2<sup>#</sup> fracturing holes. The main reason is that 3<sup>#</sup>

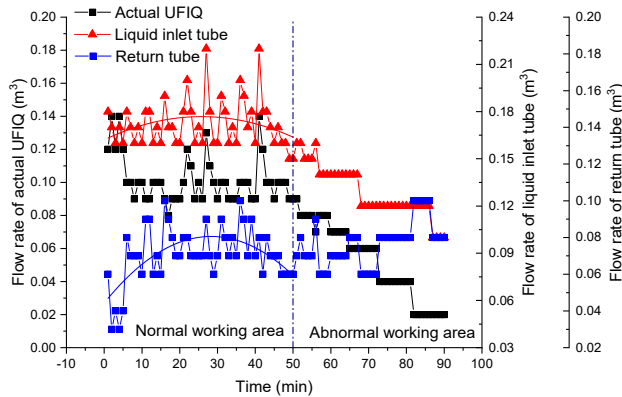


Fig. 12. Curve diagram of unit flow rate variation of 3<sup>#</sup> fracturing holes during HF

fracturing hole does not communicate with 2<sup>#</sup> control hole at 35 m on the left side through fractures until the end of HF. To facilitate the analysis, the first 50 minutes of the fracturing process of the 3<sup>#</sup> fracturing hole is also divided into normal working areas, and the last 40 minutes of the HF process is divided into abnormal working areas. In the normal working area, the change trend of the unit liquid flow rate of the liquid inlet tube, the unit liquid flow rate of the return tube and the actual UFIQ is basically the same as that of the 1~2<sup>#</sup> fracturing holes. The change trend of the unit liquid flow rate of the liquid inlet tube and the unit liquid flow rate of the return tube was “parabola” after the relevant data fitting. The change trend of actual UFIQ in the region can also be divided into decline stage and fluctuation stage. While in the abnormal working area, the unit liquid flow rate of the return tube shows an obvious upward trend, and the unit liquid flow rate of the liquid inlet tube shows a significant downward trend, while the actual UFIQ also shows a significant downward trend. The unit liquid flow rate of each pipeline in the abnormal fracturing area forms such a trend mainly because of the cracks formed by HF in the coal mass. The disturbance stress formed by the FIP at the end of the pipeline cannot overcome the minimum principal stress of the surrounding coal mass, so that the coal mass cannot crack again, and thus the overall efficiency of the emulsion pump is reduced. Most of the fracturing fluid from the water tank into the emulsion pump enters the water tank through the return tube, so the actual UFIQ entering the coal body decreases rapidly.

Coal is a porous medium, and there are natural fractures in it [31,32]. When the fracturing fluid enters the fracturing hole through the emulsion pump, under the action of the FIP, the fracturing fluid will first enter the fractures of the coal around the fracturing hole. With the increase of the FIP, the range of coal infiltration will gradually expand, but the coal infiltration efficiency will rapidly decline. Therefore, the actual UFIQ at this stage will gradually decrease. At the same time, when the liquid pressure inside the fracturing borehole reaches the minimum principal stress of the coal mass itself, the coal mass around the fracturing borehole will crack with the continuous increase of the FIP, and the cracks formed will gradually expand under the action of the liquid pressure. During this period, the liquid entering the crack will not only store energy by itself and promote crack cracking under the action of FIP, but also infiltrate the coal mass around the crack. Therefore, in this process, the UFIQ entering the coal will fluctuate back and forth with its own storage and the crack propagation of the coal mass. While when the liquid

pressure at the end of the crack cannot overcome the minimum principal stress of the surrounding coal mass itself by energy storage, the fracturing fluid entering the coal crack can only infiltrate the surrounding coal mass and cannot crack the coal mass again, so the actual UFIQ of this stage will decrease significantly.

### 3.3. Correlation Analysis between UFIQ and FIP

In the process of HF of coal seam, the FIP of different fracturing stages shows different variation laws. For example, when the coal mass cracks or cracks expand, the FIP will appear obvious “pressure relief” phenomenon, in other words, the FIP drops suddenly, and then slowly returns to the pressure value before “pressure relief”. According to the variation characteristics of FIP, we analyzed the correlation between the variation of FIP and the actual UFIQ during the whole HF process, to reveal the relationship between the two and the relationship between the variation of unit UFIQ and coal cracking and crack propagation. Throughout the HF process, 1~3<sup>#</sup> fracturing holes actual UFIQ and FIP changes as shown in Fig. 13.

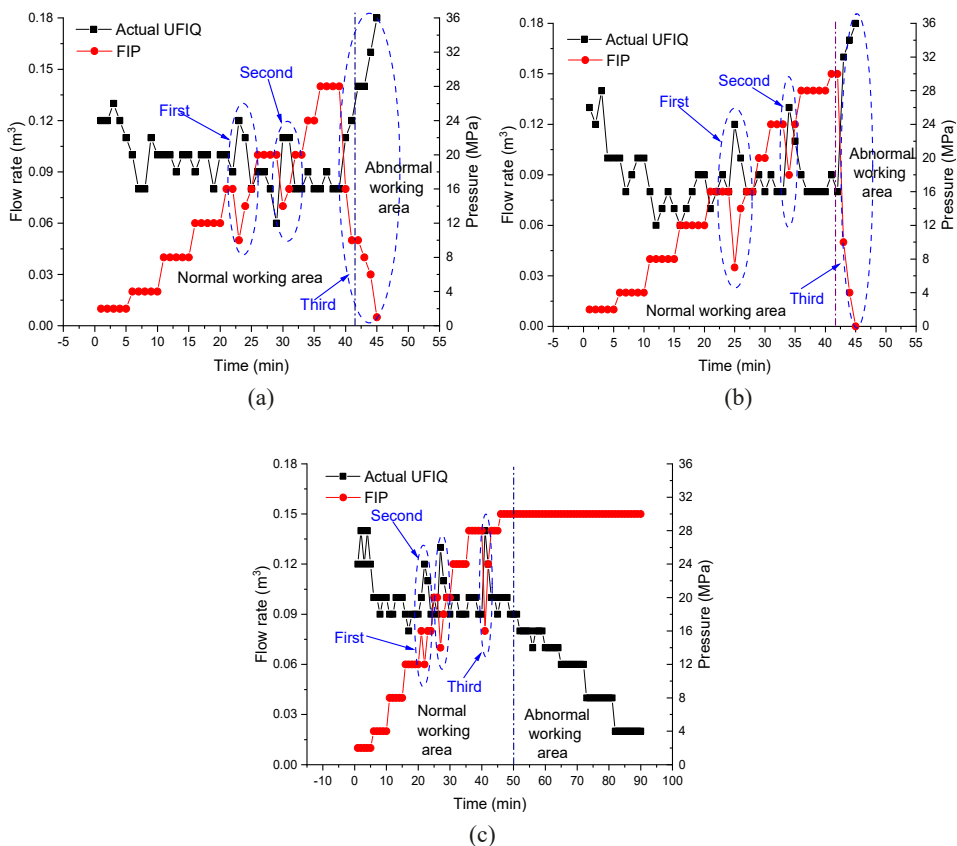


Fig. 13. The change trend diagram of UFIQ and FIP of each fracturing hole in the HF process: (a) 1<sup>#</sup> fracturing hole; (b) 2<sup>#</sup> fracturing hole; (c) 3<sup>#</sup> fracturing hole

It can be seen from Fig. 13 that there are three times of FIP “pressure relief” phenomenon in the whole fracturing process of 1~3<sup>#</sup> fracturing holes. Among them, 1<sup>#</sup> fracturing hole appeared “pressure relief” phenomenon when fracturing to 16 MPa, 20 MPa and 28 MPa, the corresponding fracturing time were 23 minutes, 30 minutes, and 40 minutes, the third time appeared “pressure relief” because 1<sup>#</sup> fracturing holes and 1<sup>#</sup> control hole through each other, so until the end of the fracturing, the FIP has been in a downward trend. When fracturing to 16 MPa, 24 MPa and 30 MPa, the 2<sup>#</sup> fracturing hole appeared “pressure relief” phenomenon, and the corresponding fracturing time were 25 minutes, 34 minutes, and 43 minutes. The third “pressure relief” was caused by the mutual penetration of 2<sup>#</sup> fracturing hole and 2<sup>#</sup> control hole. When 3<sup>#</sup> fracturing hole is fractured to 16 MPa, 20 MPa and 28 MPa respectively, the corresponding fracturing time is 22 minutes, 27 minutes, and 41 minutes respectively. The whole fracturing process of 3<sup>#</sup> fracturing hole is not communicated with other drilling holes, so each time the phenomenon of “pressure relief” is quickly restored to the level of FIP before “pressure relief”, and the FIP has not been decreased after communicating with the corresponding control holes as 1~2<sup>#</sup> fracturing holes.

Accordingly, it can also be seen from Fig. 13 that there are three obvious fluctuations in the actual UFIQ in the whole HF process of 1~3<sup>#</sup> fracturing holes, in other words, first increasing and then returning to the UFIQ level before increasing. The 1<sup>#</sup> fracturing hole appeared obvious fluctuation phenomenon when fracturing to 23 minutes, 30 minutes, and 40 minutes respectively, which was the same as the time of “pressure relief” of FIP. 2<sup>#</sup> fracturing hole in fracturing to 25 minutes, 34 minutes and 43 minutes appear obvious fluctuation phenomenon, and its FIP “pressure relief” time is the same; the 3<sup>#</sup> fracturing hole shows obvious fluctuation when fracturing to 22 minutes, 27 minutes, and 41 minutes respectively, which is also corresponding to the time of “pressure relief” of FIP. Moreover, during the HF process of 1~3<sup>#</sup> fracturing holes, the FIP shows a process from the emergence of “pressure relief” phenomenon to the recovery of the FIP level before “pressure relief”, which is basically corresponding to the process of the actual UFIQ from the emergence of an increase to the recovery of the UFIQ level before the increase, indicating that the FIP of the fracturing hole has a good correlation with the actual UFIQ during the fracturing process. When the FIP decreases significantly, the actual UFIQ will increase significantly. When the FIP is restored to the pressure value before the drop, the actual UFIQ is also restored to the level before the rise. The main reason is that when the accumulated energy value of the fracturing fluid in the coal mass is greater than the minimum stress value existing in the coal itself, the coal mass will crack and crack propagation. At this time, the fluid injection space in the coal mass will increase instantaneously. Before the fracturing fluid is not supplemented, the pressure will decrease significantly, and the pressure drop means the decrease of the pressure potential energy of the fracturing fluid. Therefore, to maintain the mechanical energy of the fracturing fluid, the kinetic energy of the fracturing fluid will increase, so that more fracturing fluid is injected into the coal mass, and then the energy is supplemented for the pressure relief fracturing fluid. With the continuous supplement of the fracturing fluid, the energy accumulated by the fracturing fluid will continue to recover to the level before the decline, and the corresponding pressure potential energy of the fracturing fluid will also increase, and then the kinetic energy of the fracturing fluid will decrease, so that the actual UFIQ will gradually recover to the original level. When the energy accumulated by the fracturing fluid at the end of the fracture reaches the level of the cracked coal mass, the above process will be recycled again until the energy accumulated by the fracturing fluid at the end of the fracture cannot make the coal mass crack, and at this time only a certain amount of fracturing fluid is needed on the coal mass surrounding the infiltration fracture, and the demand is getting smaller and smaller with

the increase of the infiltration range. Therefore, to maintain the pressure value of the fracturing fluid in the coal mass, the amount of the fracturing fluid is getting smaller and smaller, which leads to the actual UFIQ is getting smaller and smaller.

In summary, in the whole HF process of 1~3<sup>#</sup> fracturing holes, when the coal mass cracks and crack propagation, the FIP of each fracturing holes has a good correlation with the actual UFIQ, when the FIP appears obvious “decreases-recovery” phenomenon, the actual UFIQ appears obvious “rises-recovery” phenomenon, and the whole change process has synchronization. Therefore, according to the change of the actual UFIQ, it can also be used to determine whether the coal mass cracks and crack propagation, and the FIP can be adjusted according to its change. For example, when the actual UFIQ decreases significantly, it indicates that the energy provided by the FIP for the fracturing fluid is likely to have been unable to make the coal body crack, and it is necessary to increase the FIP as soon as possible to break the coal mass.

## 4. Discussion

### 4.1. Stage division of HF process

In HF of coal seam, the HF can be divided into three stages according to the variation law of unit liquid flow in different pipelines and the relationship between the actual UFIQ and FIP of each fracturing hole:

- 1) Liquid filling stage. In this stage, the FIP is low, the duration is short, and its role is mainly to inject fracturing fluid into high-pressure pipelines, boreholes, and fractures around boreholes, and gradually infiltrate coal mass around boreholes in the process of fracturing fluid entering the above space. At the same time, the connection of high-pressure pipeline and the sealing quality of fracturing hole can also be preliminarily verified by injecting fracturing fluid into the fracturing hole through low FIP. Because the FIP is generally low in this stage, it is not enough to let the fracturing fluid accumulate certain energy to make the coal mass crack, so the coal mass cracking and crack propagation will not occur in this stage.
- 2) Energy storage and coal mass cracking cycle stage. In this stage, the fracturing fluid storage is the first step, and its role is mainly to prepare for the fracturing coal. After the fracturing hole and its surrounding fractures are filled with fracturing fluid, the energy of fracturing fluid in the borehole and its surrounding fractures is continuously increased by continuously adjusting the FIP. In the process of continuous energy storage of fracturing fluid, with the gradual increase of its own energy, the scope of fracturing fluid infiltrating the surrounding coal will also increase. When the energy accumulated by the fracturing fluid is greater than the minimum principal stress existing in the coal itself, it will enter the stage of coal cracking and crack propagation. At this time, the coal will crack and crack propagation. At the same time, the FIP will appear “decreases-recovery” phenomenon, accordingly, the actual UFIQ will appear “rises-recovery” phenomenon; after the first cracking and crack propagation of coal mass, the fracturing fluid will enter the energy storage stage again. When the fracturing fluid at the end of the crack can overcome the minimum principal stress of the surrounding coal mass again, the coal mass will crack again, so it will circulate until the energy of the fracturing fluid at the end of the crack can no longer make the coal mass cracking.

- 3) Stop cracking stage. Although the fracturing fluid at the end of the crack at this stage has certain energy, its energy cannot overcome the minimum principal stress existing in the surrounding coal mass itself under the influence of crack resistance, gas pressure and in-situ stress. Therefore, the coal mass at this stage will stop cracking. At this time, the actual UFIQ will decrease significantly, especially the unit liquid flow rate of the return tube will be significantly improved. The main reason is that the coal is no longer cracking, which leads to a rapid decrease in the demand for fracturing fluid.

## 4.2. Variation characteristics of internal disturbance stress in coal mass during fracturing

After the HF of 1~2<sup>#</sup> fracturing holes was completed, each borehole stress gauge (Fig. 14) was sent to the bottom of each stress monitoring holes by using the push rod, and the hole sealing method of polyurethane-cement mortar (Fig. 15) was used to seal the hole. After the stress value of each borehole stress gauge is stable (1<sup>#</sup> stress meter value is 5.4 MPa, 2<sup>#</sup> stress meter value is 5.2 MPa, 3<sup>#</sup> stress meter value is 5.3 MPa), HF of 3<sup>#</sup> fracturing hole is started. During the whole HF process, the stress value of the borehole stress gauge and the corresponding FIP change are shown in Fig. 16.

It can be seen from Fig. 16 that in the whole HF process of 3<sup>#</sup> fracturing hole, the stress value of 1<sup>#</sup> borehole stress gauge at 10 m away from 3<sup>#</sup> fracturing hole began to rise at 19 minutes of fracturing, and the stress value was basically stable at 17.0 MPa at 48 minutes of fracturing, the stress value of 1<sup>#</sup> borehole stress gauge increased by 11.6 MPa. The stress value of the 2<sup>#</sup> borehole stress gauge at 20 m from the 3<sup>#</sup> fracturing hole began to rise after 22 minutes of fracturing, and reached a stable state after 50 minutes of fracturing, and the stress value was 14.8 MPa, the stress value of the 2<sup>#</sup> borehole stress gauge increased by 9.6 MPa; the stress value of 3<sup>#</sup> borehole stress gauge at 30 m from 3<sup>#</sup> fracturing hole is basically unchanged during the whole HF process, and the reason should be that the influence range of this HF does not reach 3<sup>#</sup> borehole stress gauge. In addition, comparing the stress values of 1<sup>#</sup> borehole stress gauge and 2<sup>#</sup> borehole stress gauge in the whole HF process, it can be seen that the disturbance stress formed by HF in coal mass decreases with the increase of the spacing between coal mass and fracturing borehole, in other words, the transmission of disturbance stress formed by HF in coal mass is mainly dominated



Fig. 14. Kse-1 mining intrinsic safety digital display borehole stress meter

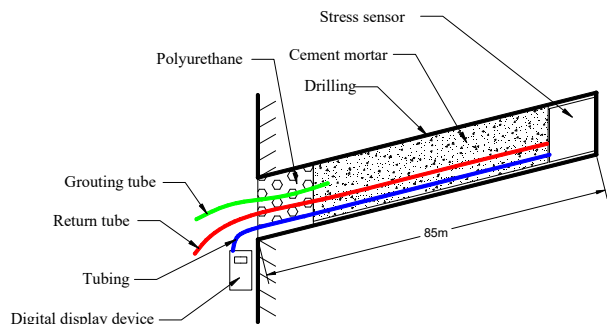


Fig. 15. Schematic diagram of polyurethane-cement mortar hole sealing

by attenuation; at the same time, according to the change of stress value of 1~2<sup>#</sup> borehole stress gauges in the whole HF process, it can be seen that in the HF process, the internal stress change process of coal mass mainly includes three stages: the original stress stage, the stress response stage and the stress stabilization stage. The value of borehole stress gauge in the original stress stage is the stress value before fracturing, currently the coal mass has not cracked, and the influence range of HF has not reached the vicinity of borehole stress gauge; the stress response stage is mainly after coal cracking, the influence range of HF reaches near the borehole stress gauge and increases rapidly with the increase of FIP. The main performance of the stress stabilization stage is that the stress value no longer changes greatly and basically tends to be stable, and the coal mass is no longer cracked at this stage.

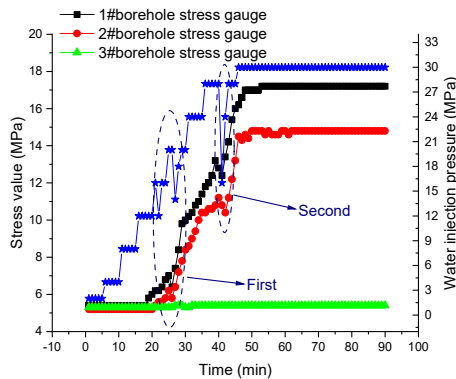


Fig. 16. Variation diagram of stress meter value of each borehole

In addition, it can also be clearly seen in Fig. 16 that the stress value of 1~2<sup>#</sup> borehole stress gauges does not show a linear growth in the stress response stage, but a wavy growth, and its fluctuation is related to the “decrease-recovery” phenomenon of FIP, which may be related to the cracking and crack propagation of coal mass. During the whole HF process, the FIP has three obvious fluctuations (decrease-recovery), and the stress value of 1~2<sup>#</sup> borehole stress gauges have two obvious fluctuations. The third fluctuation of the PIF is completely synchronized with the second fluctuation of the stress value of the 1~2<sup>#</sup> borehole stress gauges, while the first fluctuation of the stress value of the 1~2<sup>#</sup> borehole stress gauges is located between the first and second fluctuation of the FIP, and it does not show complete synchronization, which may be the reason for the short interval between the first and second fluctuation of the FIP in the HF process of the 3<sup>#</sup> fracturing hole. At the same time, according to the stress value change curve of 1~2<sup>#</sup> borehole stress gauge, when the two borehole stress gauges are within the influence range of HF, the stress value fluctuation of 1~2<sup>#</sup> borehole stress gauge is synchronous, which is mainly related to coal cracking and crack propagation.

### 4.3. Analysis of HF effect

To illustrate the permeability enhancement effect of coal seam after HF, after maintenance of return laneway and pipeline installation of 1703 mining working face were completed, 24 gas

drainage boreholes were constructed along the advancing direction of the working face in the return laneway. The hole depth is 50 m, the hole diameter is 75 mm, and the hole inclination angle is  $-14^\circ$ . The layout of each gas drainage borehole is shown in Fig. 17. After the completion of each borehole construction, the borehole sealing and grid-connected drainage were carried out immediately, and the drainage parameters of each gas drainage borehole were continuously monitored for one month. Then, it is compared with the drainage parameters of the corresponding drainage borehole in the inlet roadway. In this comparison, we mainly select the parameter of gas extraction amount. Since the number of boreholes and the extraction data are large, and the overall variation law is basically the same, five groups of corresponding gas drainage boreholes are selected respectively in the intake airflow roadway and return laneway of 1703 mining working face, and the variation law of the gas extraction amount within one month after the grid-connected drainage is compared and analyzed, as shown in Fig. 18.

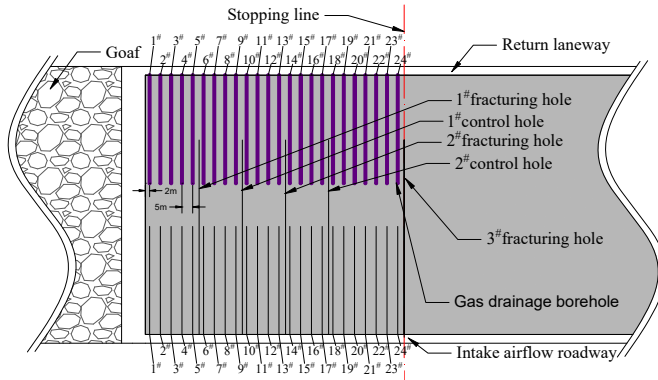


Fig. 17. Layout of gas drainage boreholes Figure

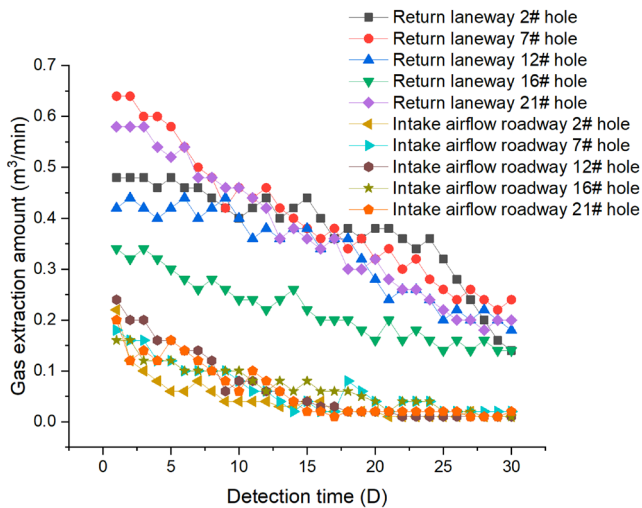


Fig. 18. The variation law of gas extraction amount in each borehole

It can be seen from Fig. 18 that after the HF coal seam permeability enhancement measures were adopted in 1703 mining working face, the gas extraction amount of gas drainage boreholes constructed in the return airway were significantly higher than the gas drainage boreholes (no HF measures were adopted) constructed in the intake airflow roadway of the working face in the detection period of 30 days of grid-connected drainage. According to the calculation, within 30 days after the grid-connected drainage of each gas drainage borehole in the intake airflow roadway, the gas extraction amount decreased from 0.16~0.22 m<sup>3</sup>/min to 0.01~0.02 m<sup>3</sup>/min, the attenuation rate was 90.91~93.75%, the average gas extraction amount was 0.04~0.07 m<sup>3</sup>/min, and the cumulative gas extraction amount was about 2028 m<sup>3</sup>. The gas extraction amount of each gas drainage borehole constructed in the return airway decreased from 0.34~0.64 m<sup>3</sup>/min to 0.14~0.24 m<sup>3</sup>/min, and the attenuation rate was 58.82~62.50%. The average gas extraction amount was 0.22~0.42 m<sup>3</sup>/min, and the cumulative gas extraction amount was about 14656 m<sup>3</sup>. Whether it is the attenuation rate of gas extraction amount, the average gas extraction amount and the cumulative gas extraction amount, the latter is better than the former, which fully shows that the effect of HF on coal seam permeability is obvious.

## 5. Conclusions

Based on engineering test, the change law of UFIQ and its correlation with FIP in the whole process of HF in coal seam are studied. And the effect of coal seam gas drainage after adopting HF anti-reflection measures is studied. The main conclusions are as follows:

- 1) In the normal HF process, the fitting curves of the variation law of the liquid flow in the inlet tube and the return tube are both “parabolas”, while the actual UFIQ can be divided into the decline stage and the fluctuation stage. The reason is mainly related to the borehole water filling, coal mass infiltration, coal mass cracking and crack propagation.
- 2) In the process of coal seam HF, there is a certain correlation between the FIP and the actual UFIQ in the process of coal mass cracking and crack propagation. The FIP will show a significant “decrease-recovery” phenomenon, while the actual UFIQ will show a “increase-recovery” phenomenon, and the two have synchronization.
- 3) According to the variation law of actual UFIQ during HF engineering test, the whole HF process is divided into three stages: liquid filling stage, energy storage and cracking cycle stage, and stop cracking stage.
- 4) The transmission of disturbance stress formed by HF in coal mass is mainly attenuation; in addition, during the whole HF process, the change process of internal disturbance stress in coal mass mainly includes three stages: the original stress stage, the stress response stage, and the stress stabilization stage.
- 5) The average gas extraction amount, attenuation rate of gas extraction amount and cumulative gas extraction amount of gas drainage boreholes in coal seam HF area are higher than those of gas drainage boreholes that are not affected by HF, indicating that HF has an obvious effect on permeability enhancement of coal seam.

### Statement

- 1) Funding: Supported by the China Scholarship Council (Grant No. 202306050102)
- 2) Competing Interests: The authors have no relevant financial or non-financial interests to disclose.

## References

- [1] K. Wang, F. Du, Coal-gas compound dynamic disasters in China: A review. *Process Saf. Environ.* **133**, 1-17 (2020). DOI: <https://doi.org/10.1016/j.psep.2019.10.006>
- [2] F.B. Zhou, T.Q. Xia, X.X. Wang, Y.F. Zhang, Y.N. Sun, J.S. Liu, Recent developments in coal mine methane extraction and utilization in China: A review. *J. Nat. Gas. Sci. Eng.* **31**, 437-458 (2016). DOI: <https://doi.org/10.1016/j.jngse.2016.03.027>
- [3] H. Yang, J.Z. Liu, D.M. Zhang, W.J. Xiao, X.L. Wang, K. Wang, Response Characteristics of Coal Measure Strata Subjected to Hydraulic Fracturing: Insights from a Field Test. *Energ. Fuel.* **35**, 19410-19422 (2021). DOI: <https://doi.org/10.1021/acs.energyfuels.1c02791>
- [4] X.G. Wang, Q.T. Hu, Q.G. Li, Investigation of the stress evolution under the effect of hydraulic fracturing in the application of coalbed methane recovery. *Fuel* **300**, 120930 (2021). DOI: <https://doi.org/10.1016/j.fuel.2021.120930>
- [5] X.F. Li, H.B. Li, L. W. Liu, Y.Q. Liu, M.H. Ju, J. Zhao, Investigating the crack initiation and propagation mechanism in brittle rocks using grain-based finite-discrete element method. *Int. J. Rock Mech. Min.* **127**, 104219 (2020). DOI: <https://doi.org/10.1016/j.ijrmms.2020.104219>
- [6] X.J. Hao, Y.N. Wei, K. Yang, J. Sun, Y.F. Sun, G.P. Zhu, S.H. Wang, H.B. Chen, Z.W. Sun, Anisotropy of crack initiation strength and damage strength of coal reservoirs. *Petrol. Explor. Dev.* **48**, 243-255 (2021). DOI: [https://doi.org/10.1016/S1876-3804\(21\)60020-4](https://doi.org/10.1016/S1876-3804(21)60020-4)
- [7] X.G. Kong, E.Y. Wang, S.G. Li, H.F. Lin, Z.B. Zhang, Y.Q. Ju, Dynamic mechanical characteristics and fracture mechanism of gas-bearing coal based on SHPB experiments. *Theor. Appl. Fract. Mec.* **105**, 102395 (2020). DOI: <https://doi.org/10.1016/j.tafmec.2019.102395>
- [8] C.P. Xin, F. Du, K. Wang, C. Xu, S.G. Huang, J.T. Shen, Damage evolution analysis and gas–solid coupling model for coal containing gas. *Geomech. Geophys. Geo.* **7**, 7 (2021). DOI: <https://doi.org/10.1007/s40948-020-00205-6>
- [9] H.F. Wang, Y.P. Cheng, L. Yuan, Gas outburst disasters and the mining technology of key protective seam in coal seam group in the Huainan coalfield. *Nat. Hazards* **67**, 763-782 (2013). DOI: <https://doi.org/10.1007/s11069-013-0605>
- [10] L. Li, J.Q. Tan, D.A. Wood, Z.G. Zhao, Q. Lyu, B. Shu, H.C. Cheng, A review of the current status of induced seismicity monitoring for hydraulic fracturing in unconventional tight oil and gas reservoirs. *Fuel* **242**, 195-210 (2019). DOI: <https://doi.org/10.1016/j.fuel.2019.01.026>
- [11] L.G. Wang, Y.P. Xu, Study of the law of gradual change of the influence of hydraulic punching under a rational coal output. *Arab. J. Geosci.* **12**, No. 427 (2019). DOI: <https://doi.org/10.1007/s12517-019-4577-8>
- [12] T. Liu, B.Q. Lin, Q.L. Zou, C.J. Zhu, Microscopic mechanism for enhanced coal bed methane recovery and outburst elimination by hydraulic slotting: A case study in Yangliu mine, China. *Greenh. Gases.* **6**, 597-614 (2016). DOI: <https://doi.org/10.1002/ghg.1591>
- [13] Y.P. Cheng, Z.H. Lu, X.D. Du, X.F. Zhang, M.R. Zeng, A Crack Propagation Control Study of Directional Hydraulic Fracturing Based on Hydraulic Slotting and a Nonuniform Pore Pressure Field. *Geofluids* **13** (2020). DOI: <https://doi.org/10.1155/2020/8814352>
- [14] X. Bai, D.M. Zhang, S. Zeng, S.W. Zhang, D.K. Wang, F.L. Wang, An enhanced coalbed methane recovery technique based on CO<sub>2</sub> phase transition jet coal-breaking behavior. *Fuel* **265**, 116912 (2020). DOI: <https://doi.org/10.1016/j.fuel.2019.116912>
- [15] X.H. Zhou, X.L. Li, G. Bai, D.C. Bi, W.T. Liu, An experimental investigation of the effect of acid stimulation on gas extraction from coal. *AIP Adv.* **10**, No. 115309 (2021). DOI: <https://doi.org/10.1063/5.0020650>
- [16] W.Y. Lu, B.X. Huang, X.L. Zhao, A review of recent research and development of the effect of hydraulic fracturing on gas adsorption and desorption in coal seams. *Adsorpt. Sci. Technol.* **37**, 509-529 (2019). DOI: <https://doi.org/10.1177/0263617419857400>
- [17] H. Li, M.J. Liu, H.W. Yang, H. Gao, T.Q. Xia, Influence range simulation of loose blasting borehole in the coal-rock mass. *Therm. Sci.* **23**, 4157-1464 (2019). DOI: <https://doi.org/10.2298/tsci180607211L>
- [18] Q.T. Hu, L. Liu, Q.G. Li, Y.Q. Wu, X.G. Wang, Z.Z. Jiang, F.Z. Yan, Y.C. Xu, X.B. Wu, Experimental investigation on crack competitive extension during hydraulic fracturing in coal measures strata. *Fuel* **265**, No. 117003 (2020). DOI: <https://doi.org/10.1016/j.fuel.2019.117003>

- [19] L. Zhuang, S.G. Juang, M. Diaz, K.Y. Kin, H. Hofmann, K.B. Min, A.R. Zang, O. Stephansson, G. Zimmermann, J.S. Yoon, Laboratory True Triaxial Hydraulic Fracturing of Granite Under Six Fluid Injection Schemes and Grain-Scale Fracture Observations. *Rock Mech. Rock Eng.* **53**, 4329-4344 (2020). DOI: <https://doi.org/10.1007/s00603-020-02170-8>
- [20] W.G.P. Kumari, P.G. Ranjith, M.S.A. Perera, X. Li, L.H. Li, B.K. Chen, B.L. Avabthi Isaka, V.R.S. De Silva, Hydraulic fracturing under high temperature and pressure conditions with micro CT applications: Geothermal energy from hot dry rocks. *Fuel* **230**, 138-154 (2018). DOI: <https://doi.org/10.1016/j.fuel.2018.05.040>
- [21] T. Ito, K. Hayashi, Analysis of crack reopening behavior for hydrofrac stress measurement. *Int. J. Rock Mech. Min.* **30**, 1235-1240 (1993). DOI: [https://doi.org/10.1016/0148-9062\(93\)90101-1](https://doi.org/10.1016/0148-9062(93)90101-1)
- [22] F.S. Zhang, Branko. Damjanac, Shawn. Maxwell, Investigating Hydraulic Fracturing Complexity in Naturally Fractured Rock Masses Using Fully Coupled Multiscale Numerical Modeling. *Rock Mech. Roc.k Eng.* **52**, 5137-5160 (2019). DOI: <https://doi.org/10.1007/s00603-019-01851-3>
- [23] C. Lin, J. Mao, J. He, X. Li, J. Zhao, Propagation characteristics and aperture evolution of hydraulic fractures in heterogeneous granite cores. *Arab. J. Geosci.* **12**, 684 (2019). DOI: <https://doi.org/10.1007/s12517-019-4887-x>
- [24] B.B. Zhang, B. Li, D.W. Zhang, J.J. Li, Experimental research on permeability variation from the process of hydraulic fracturing of high-rank coal. *Environ. Earth Sci.* **79**, 45 (2020). DOI: <https://doi.org/10.1007/s12665-019-8764-4>
- [25] K. Shan, Y.J. Zhang, Y.H. Zheng, Y.X. Cheng, Y.X. Yang, Effect of fault distribution on hydraulic fracturing: Insights from the laboratory. *Renew. Energ.* **163**, 1817-1830 (2021). DOI: <https://doi.org/10.1016/j.renene.2020.10.083>
- [26] M.Z. Gao, J. Xie, J. Guo, Y.Q. Lu, Z.Q. He, C. Li, Fractal evolution and connectivity characteristics of mining-induced crack networks in coal masses at different depths. *Geomech. Geophys. Geo.* **7**, 9 (2021). DOI: <https://doi.org/10.1007/s40948-020-00207-4>
- [27] T.H. Yang, J. Liu, W.C. Zhu, D. Elsworth, L.G. Tham, C.A. Tang, A coupled flow-stress-damage model for groundwater outbursts from an underlying aquifer into mining excavations. *Int. J. Rock Mech. Min.* **44**, 87-97 (2007). DOI: <https://doi.org/10.1016/j.ijrmms.2006.04.012>
- [28] Y.P. Cheng, Z.J. Pan, Reservoir properties of Chinese tectonic coal: A review. *Fuel* **260**, 116350 (2020). DOI: <https://doi.org/10.1016/j.fuel.2019.116350>
- [29] H. Gan, S.P. Nandi, P.L. Walker, Jr, Nature of the porosity in American coals. *Fuel* **51**, 27277 (1972). [https://doi.org/10.1016/0016-2361\(72\)90003-8](https://doi.org/10.1016/0016-2361(72)90003-8)
- [30] G.Z. Zhao, B.S. Zhang, L.H. Zhang, C. Liu, S. Wang, Roof Fracture Characteristics and Strata Behavior Law of Super Large Mining Working Faces. *Geofluids* **2021**, 8530009 (2021). DOI: <https://doi.org/10.1155/2021/8530009>
- [31] T. Wang, W.R. Hu, D. Elsworth, W. Zhou, X.Y. Zhao, L.Z. Zhao, The effect of natural fractures on hydraulic fracturing propagation in coal seams. *J. Petrol. Sci. Eng.* **150**, 180-190 (2017). DOI: <https://doi.org/10.1016/j.petrol.2016.12.009>
- [32] D.G. Crosby, M.M. Rahman, M.K. Rahman, S.S. Rahman, Single and multiple transverse fracture initiation from horizontal wells. *J. Petrol. Sci. Eng.* **35**, 191-204 (2002). DOI: [https://doi.org/10.1016/S0920-4105\(02\)00243-7](https://doi.org/10.1016/S0920-4105(02)00243-7)